sciendo

Influence of bath temperature on microstructure and NH$_3$ sensing properties of chemically synthesized CdO thin films

A.K. Sharma[1], S.S. Potdar[2,*], M.A. Yewale[3], Deepak B. Shirgaonkar[4], K.S. Pakhare[5], B.M. Sargar[6], M.V. Rokade[7], U.M. Patil[8]

[1]School of Physics, Shri Mata Vaishnodevi University, Kakryal, Katra-182320, J&K, India

[2]Department of Physics, Sanjeevan Engineering and Technology Institute, Panhala-416201, MS, India

[3]Department of Physics, New Arts, Commerce and Science College, Parner, Ahmednagar, MS, India

[4]Department of Physics, Ashokrao Mane Group of Institution, Vathar, Kolhapur, MS, India

[5]Department of Chemistry, Anandibai Raorane Art, Commerce and Science College, Vaibhavwadi, MS-416810, India

[6]Material Science Research Laboratory, Department of Chemistry, Jaysingpur College, Jaysingpur, MS -416101, India

[7]Semiconductor Laboratory, Centre for Materials for Electronics Technology (C-MET), IDA Phase-III, Cherlapally, HCL (PO), Hyderabad-500051, India

[8]Centre for Interdisciplinary Research, D.Y. Patil Education Society (Deemed to be University), Kolhapur-416006, India

Cadmium oxide (CdO) thin films were synthesized using chemical bath deposition (CBD) method from aqueous cadmium nitrate solution. The bath temperatures were maintained at room temperature (25 °C) and at higher temperature (80 °C). The structural studies revealed that the films showed mixed phases of CdO and Cd(OH)$_2$ with hexagonal/monoclinic crystal structure. Annealing treatment removed the hydroxide phase and the films converted into pure CdO with cubic, face centered crystal structure. SEM micrographs of as-deposited films revealed nanowire-like morphology for room temperature deposited films while nanorod-like morphology for high temperature deposited films. However, cube-like morphology was observed after air annealing. Elemental composition was confirmed by EDAX analysis. Band gap energies of the as-deposited films varied over the range of 3 eV to 3.5 eV, whereas the annealed films showed band gap energy variation in the range of 2.2 eV to 2.4 eV. The annealed films were successfully investigated for NH$_3$ sensing at different operating temperatures and at different gas concentrations. The room temperature synthesized film showed a response of 17.3 %, whereas high temperature synthesized film showed a response of 13.5 % at 623 K upon exposure to 24 ppm of NH$_3$.

Keywords: *CdO thin films; chemical bath deposition; X-ray diffraction; scanning electron microscopy; optical properties; EDAX; gas sensing*

1. Introduction

Detection of toxic gases, pollutants, combustive and process gases is important for system and process control, safety monitoring and environmental protection. Traditional analysis methods used in gas sensing include gas chromatography, Fourier-transform, infrared spectroscopy, mass spectrometry etc. These methods are complex and also require sample preparation, so that on-line, real-time analysis is difficult. However, gas sensors based on solid state semiconductor materials offer considerable advantages over other gas sensing methods. The great interest of industrial and scientific fields in semiconductor oxide gas sensors comes from their numerous advantages, such as small size, improved sensitivity towards low concentrations (at a level of ppm or even ppb) for a wide range of gaseous chemical compounds, possibility of on-line monitoring and low cost. Also, semiconductor sensors are easy to miniaturize, robust, reliable, and can be designed to operate over a range of conditions including high temperatures. Semiconductor sensors can be produced in arrays to allow sensing of multiple species simultaneously. Transparent semiconducting

*E-mail: sachinpotdar20@gmail.com

oxides found different fields of applications such as flat panel displays, smart windows, light emitting diodes, electronic and photovoltaic devices [1–4]. Cadmium oxide has direct band gap of 2.2 eV to 2.5 eV [5] and indirect band gap of 1.36 eV to 1.98 eV [6–8]. It is an n type semiconductor with rock-salt crystal structure. The synthesis of nanocrystalline materials with organized morphologies is always very important. Bath temperature is one of crucial parameter in chemical bath deposition which affects the surface morphology and the microstructure of the films [9]. CdO thin films were obtained by using several techniques such as spray pyrolysis [10], DC magnetron sputtering [11], sol-gel [12], chemical vapor deposition [13] and chemical bath deposition (CBD) [14], etc. Amongst the above mentioned methods, CBD has its own advantages, such as simplicity, reproducibility, environmental friendliness, cost-effectiveness, etc. It is a low temperature method and it does not require any sophisticated instruments as well as it is well suited for producing large-area thin films. It involves deposition of semiconductor thin film on various types of substrates that are kept in aqueous solutions.

With the above considerations, we report the effect of bath temperature on the structural, morphological and optical properties of nanocrystalline CdO thin films chemically deposited from aqueous alkaline nitrate bath. As-deposited films were annealed at 450 °C for 2 h in a muffle furnace to obtain CdO films. The as-deposited and annealed films were characterized by X-ray diffraction (XRD), scanning electron microscope (SEM), UV-Vis spectrophotometry for their structural, surface morphological and optical analysis. The elemental analysis was performed by energy dispersive X-ray analysis (EDAX).

2. Experimental

Synthesis of CdO thin films was carried out by using CBD method which is based on stirring of alkaline bath of cadmium salt containing the substrates immersed in it. In a typical experimental procedure, 0.1 M $Cd(NO_3)_2$ was used as a source of cadmium and, aqueous ammonia solution was added under constant stirring to make it alkaline. At first, the solution became milky-turbid due to the formation of $Cd(OH)_2$ precipitate. Further addition of excess ammonia dissolved the turbidity and made the solution clear and transparent. The pH of the resultant solution was ~12. The glass microslides were cleaned with a soap solution and chromic acid and then subsequently washed with double distilled water followed by ultrasonically cleaning for 15 min. The cleaned substrates were immersed vertically in the bath at room temperature under constant stirring. Precipitation took place in the bath. During the precipitation, heterogeneous reaction occurred and the deposition of CdO on the substrate took place. The substrates were removed from the bath and washed with double distilled water, dried in air and preserved in an airtight container. The obtained films were uniform and well adherent to the substrates. Similarly, another bath was prepared by maintaining the same preparative parameters as stated above but its temperature was 80 °C. Uniform and homogeneous films were obtained. The obtained films at room temperature as well as at 80 °C were annealed in the muffle furnace at 450 °C for 2 h. The film prepared at room temperature was named as A1, while the annealed film as A2. In similar way, the film prepared at higher temperature was named as C1 and annealed film as C2. To study the structural properties of as-deposited and annealed films, X-ray diffraction patterns were recorded using X-ray diffractometer over 2θ (scanning angle range of 20° to 80° with CuKa radiation). Surface morphological studies were carried out using scanning electron microscopy. Optical absorption was measured over the wavelength range of 350 nm to 850 nm using a UV-Vis spectrophotometer. Energy dispersive X-ray analysis (EDAX) was employed for the compositional studies. The gas sensing properties of synthesized films were studied using a "static gas-sensing system". There was electrical feed through the base plate. The heater was fixed below the base plate to heat the sample under test up to required operating temperatures. An Al-Cr thermocouple was used to sense

the operating temperature of the sensors. The output of the thermocouple was connected to digital temperature indicators. A gas inlet valve was provided at one port of the base plate. The required gas concentration inside the static system was attained by injecting a known volume of test gas using a gas-injecting syringe. For electrical measurements, silver paste contacts were made on the sample of area 1 cm × 1 cm. Initially, the I-V characteristics were studied within ±10 V and it was found that in this voltage range, the silver contacts showed ohmic behavior. The electrical resistance of the films in air R$_a$ and in the presence of test gas R$_g$ was measured to evaluate the gas response, S, defined as follows:

$$S\,(\%) = \frac{R_a - R_g}{R_a} \times 100 \qquad (1)$$

3. Results and discussion
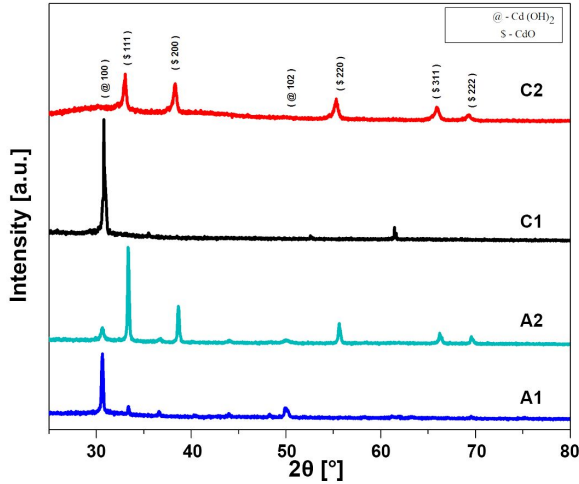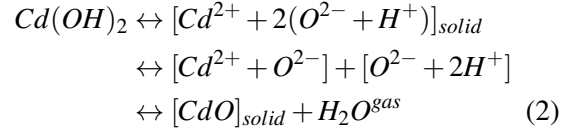
3.1. XRD analysis

Fig. 1. X-ray diffraction patterns of films deposited at room temperature - A1 and 80 °C - C1 and annealed samples A2 and C2 corresponding to A1 and C1 thin films.

The structural changes and identification of phases of CdO thin films obtained by CBD were investigated with the help of X-ray diffraction (XRD). The diffraction angle 2θ was varied between 20° and 80° and the recorded XRD patterns for all the thin films are shown in Fig. 1. It is clear

that the as-deposited samples (A1 and C1) are oriented along (1 0 0) plane which corresponds to hexagonal CdO/Cd(OH)$_2$ structure. After annealing, Cd(OH)$_2$ films converted to pure CdO as per the following reaction [15]:

$$Cd(OH)_2 \leftrightarrow [Cd^{2+} + 2(O^{2-} + H^+)]_{solid}$$
$$\leftrightarrow [Cd^{2+} + O^{2-}] + [O^{2-} + 2H^+]$$
$$\leftrightarrow [CdO]_{solid} + H_2O^{gas} \qquad (2)$$

XRD patterns of annealed films show polycrystalline nature with the most prominent orientations along (1 1 1) and (2 0 0) planes. The diffraction peak at 34° corresponds to the (1 1 1) plane of the cubic CdO phase. The presence of diffraction peaks shows a cubic, face centered structure with polycrystalline nature. The observed d values of the film were in good agreement with those reported in the JCPD data file for CdO (JCPDS File No. 31-228, 01-1049). The crystallite size (D) of CdO thin films prepared at different bath temperatures was calculated from X-ray diffraction studies using the following equation:

$$D = \frac{0.9\lambda}{\beta \cos \theta} \qquad (3)$$

where β is the half width of diffraction peak measured in radian. The crystallite size calculated by using the above formula for the sample prepared at room temperature was 42 nm and for the sample prepared at higher temperature it was 69 nm. The increase in particle size at higher temperature might be due to the fact that the nuclei formed initially might be dissolved at this temperature and thus the number of the nuclei was reduced. As there was more reactant per nucleus, the particle size increased.

3.2. SEM and EDAX analysis

Fig. 2 shows SEM images of as-deposited and annealed CdO thin films deposited at room temperature and at 80 °C. The SEM micrograph of as-deposited films shows nanowire- (sample A1) and nanoflake- (sample C1) like morphologies as shown in Fig. 2a, Fig. 2b, Fig. 2e, and Fig. 2f. It reveals that the as-deposited films both at room
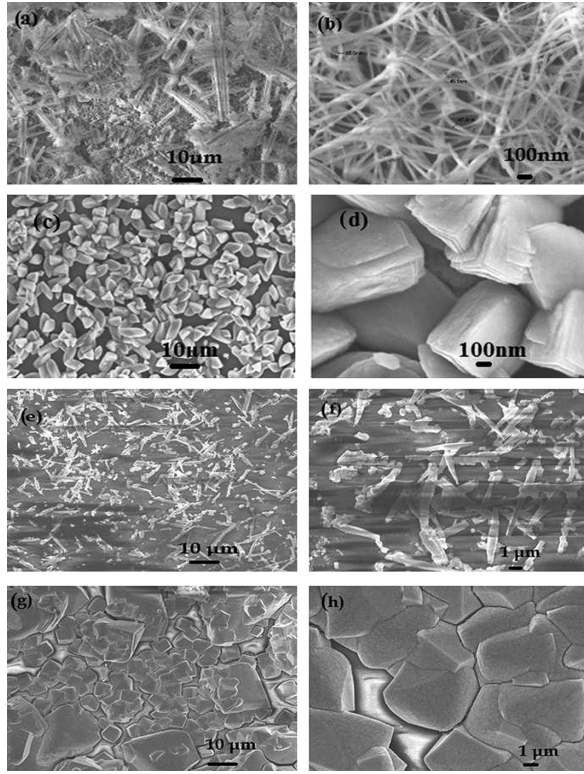
Fig. 2. SEM images of the films deposited at room temperature (a, b) and at 80 °C temperature (e, f) and their annealed (c, d and g, h) counterparts.
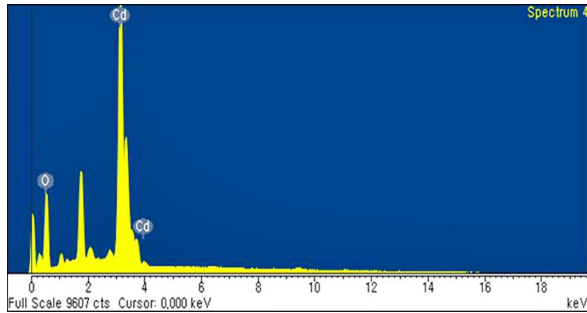

Fig. 3. Energy dispersive X-ray analysis spectrum for the CdO thin film.

temperature and 80 °C contain mixed phase of $Cd(OH)_2$ and CdO which is also shown by XRD. The annealed films show a cube-like morphology for sample A2 and sample C2 which extends on the whole surface (Fig. 2c, Fig. 2d, and Fig. 2g, Fig. 2h at various magnifications). The samples were characterized by an energy dispersive X-ray analyzer to find the elemental composition of the films. Fig. 3

Table 1. Elemental composition of the CdO thin film.

Serial no.	Element	wt.%	at.%
1	O K	45.33	85.35
2	Cd L	54.67	14.65
	Total	100	100

and Table 1 show the elemental composition of the CdO films formed by CBD method. It is clearly seen that the atomic percentages of Cd and O are 14.65 and 85.35, respectively. The results indicate the presence of high concentration of oxygen.

3.3. Optical studies

The plots of $(\alpha h\nu)^2$ versus $h\nu$ for the as-deposited and annealed films are shown in Fig. 4(a, b). The absorption spectra of as-deposited and annealed films deposited at room temperature and 80 °C were studied without taking into account the reflection and transmission losses. Annealing in the muffle furnace might cause oxidizing any hydroxide to oxide and it may explain the effect of annealing on optical absorption. It is obvious that the as-deposited films show the band gap in the range of 3 eV to 3.5 eV. Such blue shifting may be due to the presence of high bandgap hydroxide phase in both the as-deposited samples. Furthermore, from XRD patterns it is also seen that the as-deposited films (sample A1 and sample C1) consist of a mixture of different phases - cubic CdO and monoclinic/hexagonal $Cd(OH)_2$. It may explain why both the films show blue shift of more than 1.2 eV [16]. The decrease in the band gap observed after annealing may be due to the fact that the removal of $Cd(OH)_2$ from the film took place. Band gap of 2.4 eV (sample A2) and 2.3 eV (sample C2) was evaluated. Many researchers have reported a decrease in band gap after annealing [17] for chemically deposited metal oxide thin films due to removal of hydroxide phase. These values are in good agreement with observed band gap values of CdO (2.2 eV to 2.5 eV).
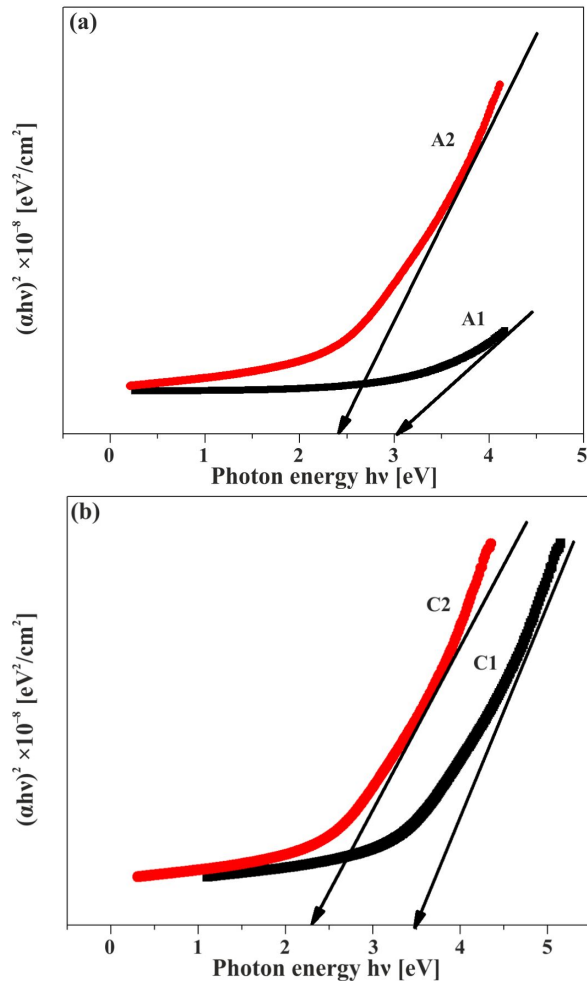
Fig. 4. The plots of $(\alpha h\nu)^2$ against $h\nu$ for (a) film deposited at room temperature (A1) and annealed film (A2), (b) film deposited at 80 °C (C1) and annealed film (C2).

3.4. Gas sensing properties

3.4.1. Effect of temperature

Before exposing to NH₃ gas, the CdO films were allowed to stabilize in terms of electrical resistance for half an hour and the stabilized resistance was taken as R_a. Initially, the gas response was studied as a function of operating temperature for annealed CdO film. The temperature of the sensor surface is one of the most important parameters. The temperature affects the physical properties of the semiconductor sensor material, such as charge carrier concentration, Debye length, work function, etc. The optimum operating temperature for an effective sensor performance corresponds to that, where the material is able to catalytically reduce or oxidize the target gas, simultaneously changing the electrical properties of the sensor material. Response of sensors depends on two factors, namely, the speed of chemical reaction on the surface of the grains, and the speed of diffusion of gas molecules to that surface. These are activation processes, and the activation energy of chemical reactions is high. At low temperatures, the sensor response is restricted by the speed of chemical reactions. At higher temperature the sensor response is restricted by the speed of diffusion of gas molecules to that surface. At some intermediate temperature, speed values of the two processes become equal, and at that point the sensor response reaches its maximum [18]. According to this mechanism there is a certain temperature for every gas at which the sensor response reaches its peak value. Above this maximum temperature, the gas response decreases due to desorption of the oxygen which has been adsorbed on the surface of the sensor [19]. Another reason for the decrease in the gas response above the maximum temperature could be the increase in the carrier concentration due to intrinsic thermal excitation which decreases the Debye length [20]. This length describes the size of the space-charge region next to the surface where the free carrier concentration may be affected by the surface species. In addition, humidity also plays an important role in sensing performance. As we know, water adsorbing on the metal oxide surface does not give electrons to sensing layers. However, as explained in the literature [21, 22], it reduces the sensitivity of metal oxide sensors due to the reaction between the surface oxygen and the water molecules, which results in the decrease in baseline resistance of the gas sensor, and consequently decrease in the sensitivity [22]. Secondly, the adsorption of water molecules leads to reduced chemisorption of oxygen species on the oxide surface due to the decrease of surface area that is responsible for the sensor response. However, surface hydroxyls start to desorb at higher temperatures [23] and the hydroxyl ions can be removed by heating sensor surface at higher temperatures. Hence, recovery of

baseline resistance can be achieved. Thus, humidity effect depends on the reaction temperature of sensor becoming small at temperatures above 350 °C. In the present case we found that the sensor response reaches maximum at 623 K with negligible impact of humidity. Fig. 5(a, b) shows the influence of humidity on sensing performance and it is observed that the performance reduces from ∼20 % to ∼17 % due to humidity impact for sample A2. Considering the influence of humidity, the gas response of sample C2 and sample A2 (RT) was observed to be 13.5 % and 17.3 %, respectively (shown in Fig. 5b).
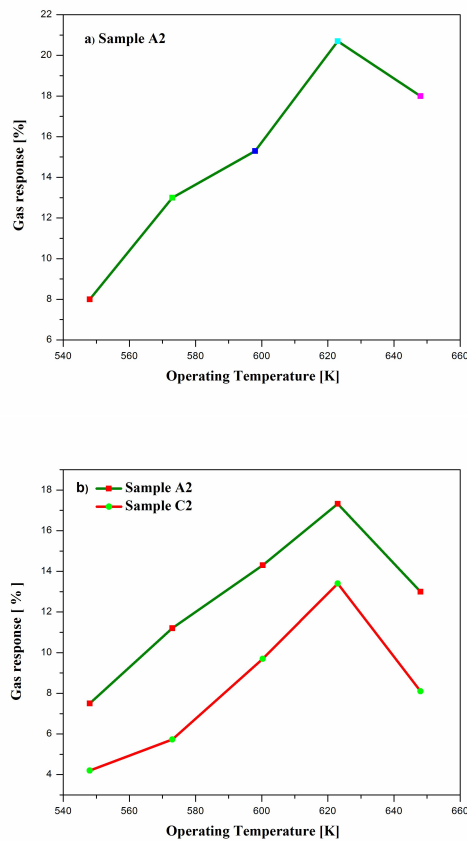

Fig. 5. Plots of gas response as a function of operating temperature for samples A2 and C2: (a) in dry air (b) at 30 % relative humidity RH.

Once the operating temperature was fixed, the sensor response was studied at different gas concentrations.

3.4.2. Effect of NH$_3$ concentration

Fig. 6(a, b) reveals that the response increased from 12.5 % to 19.8 % for the sample deposited at room temperature (A2), while from 7.2 % to 14.5 % for the sample deposited at 80 °C as the NH$_3$ concentration increased from 16 ppm to 28 ppm. However, at higher concentrations the increase in gas response value was steady and saturated.
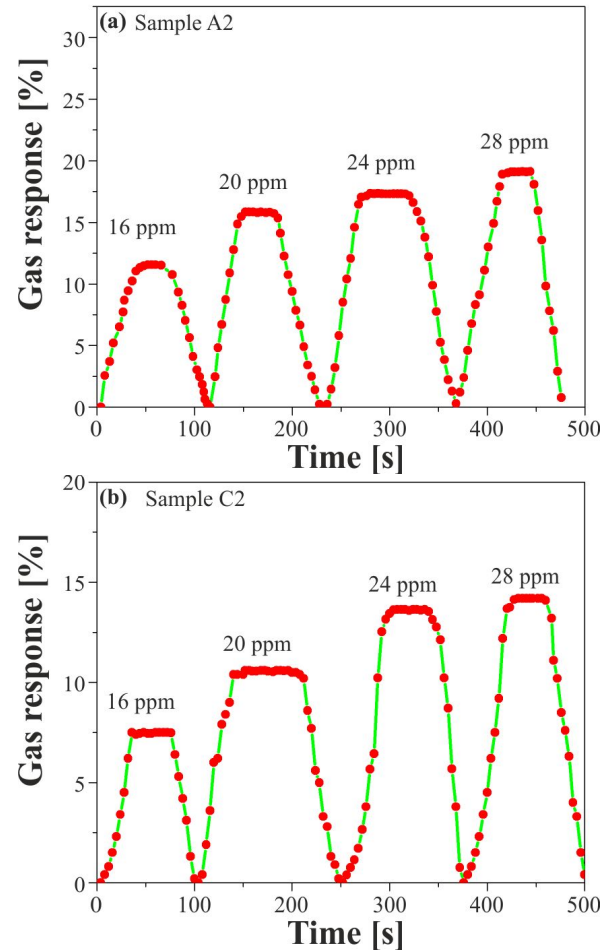

Fig. 6. Transient gas response under different gas concentrations for (a) sample A2 (b) sample C2.

The response of a sensor mostly depends on the removal of adsorbed oxygen molecules by reaction with a target gas and generation of electrons. For a small concentration of gas, acting on a fixed surface area of a sample, there is a low coverage of gas molecules on the surface and hence, minor surface reaction takes place. An increase in gas
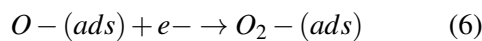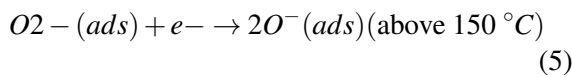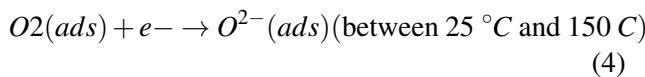
concentration increases the surface reaction due to a larger surface coverage. A further increase in surface reaction is gradual when the saturation point of the coverage of molecules is reached.

3.4.3. Effect of bath temperature

Fig. 7 (a, b) shows the gas response of CdO films obtained by chemical bath deposition method at different bath temperatures upon exposure to 24 ppm of NH₃ gas at 623 K. The figure shows that the gas response of 13.5 % was obtained for the sample deposited at 80 °C (C2) whereas the response of 17.3 % was obtained for the sample deposited at room temperature (A2). It is evident that the response largely depends upon particle size. Sample A2 with average grain size of 42 nm (as confirmed by XRD) is more sensitive than sample C2. Furthermore, A2 is composed of porous nanocubes (it is also visible in SEM), which offer more surface area for interaction with NH₃ molecules and enhance diffusion process.

3.4.4. Discussion

The mostly accepted theory for the mechanism of gas sensing of n-type semiconducting metal oxide is based on the electron transport between the sensor surface and chemisorbed species that modify the surface conductivity of the sensor [24]. When the sensor is exposed to air, the atmospheric oxygen molecules are adsorbed on the surface of the sensor, and then capture electrons from the conduction band to form the chemisorbed oxygen species (O^{2-}, O^{-}, O_2-):

$$O2(ads) + e- \rightarrow O^{2-}(ads) \text{(between 25 °C and 150 C)} \quad (4)$$

$$O2-(ads) + e- \rightarrow 2O^{-}(ads) \text{(above 150 °C)} \quad (5)$$

$$O-(ads) + e- \rightarrow O_2-(ads) \quad (6)$$

Therefore, the adsorbed oxygen molecules act as acceptors and thus deplete the surface electron states and reduce the free carrier density, which subsequently results in formation of electron depletion region at the surface of the sensor. Once the
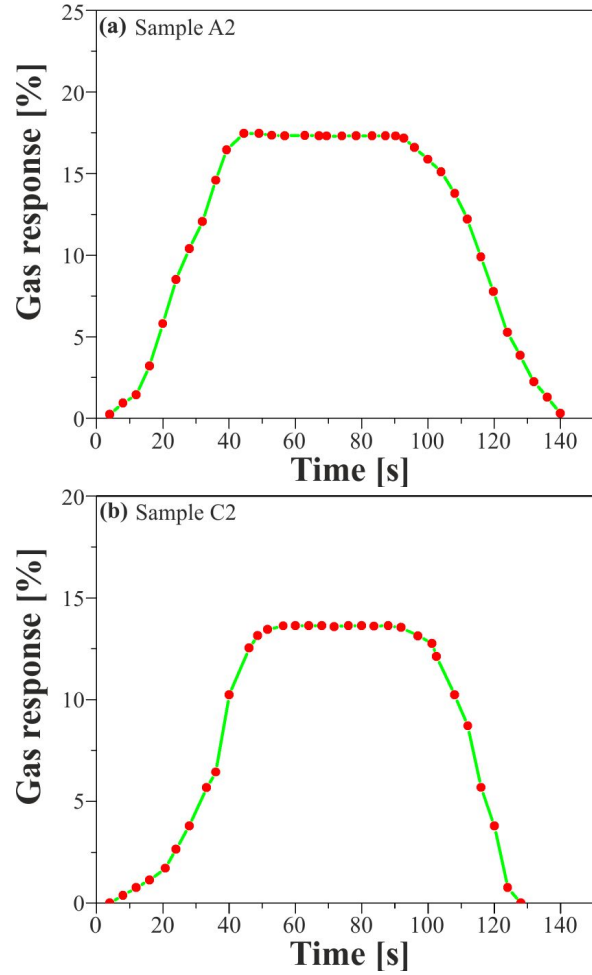

Fig. 7. Transient gas response 24 ppm of NH₃ at 623 K for (a) sample A2, (b) sample C2.

sensor is exposed to a target gas, the reaction between the analyte gas molecules and adsorbed oxygen species will occur. It releases electrons back to the conduction band of material. The released free electrons recombine with holes, which increases the electrical conductance of the semiconductor. These processes can be described by the following reactions:

$$4NH_3 + 3O^{2-}(ads) \rightarrow 2N_2 + 6H_2O + 6e^{-} \quad (7)$$
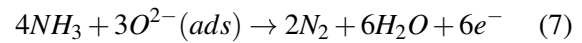
4. Conclusions

The CdO thin films were deposited by using chemical method at room temperature as well as at temperature of 80 °C. As-deposited films

showed mixed phases of CdO and Cd(OH)$_2$ with hexagonal/monoclinic crystal structure whereas the annealed films showed face centered cubic crystal structure. SEM investigations revealed the nanowire-like morphology for the room temperature deposited film and well-developed rod-like morphology for the film deposited at elevated temperature. Annealed samples showed the cube-like morphology. Optical studies indicated that the band gap energy Eg of as-deposited films varied in the range of 3 eV to 3.5 eV. After annealing, the band gap decreased to 2.4 eV for room temperature deposited film and 2.3 eV for high temperature deposited film. EDAX analysis showed the presence of high concentration of oxygen. The sensing properties of CdO thin films prepared at different bath temperatures were studied systematically and it was found that the film deposited at room temperature showed response of 17.3 %, while the film deposited at higher temperature showed response of 13.5 % to 24 ppm of NH$_3$ at 623 K.

References

[1] LEWIS B.G., PAINE D.C., *MRS Bull.,* 25 (2000), 22.

[2] KIM H., GILMORE C.M., PIQUE A., HORWITZ J.S., MATTOUSSI H., MURATA H., KAFAFI Z.H., CHRISEY D. B., *J. Appl. Phys.,* 86 (1999), 6451.

[3] SELVAN J.A.A., DELAHOY A.E., GUO S., LI Y.M., *Sol. Energ. Mat. Sol. C.,* 90 (2006), 3371.

[4] ANANDAN S., *Curr. Appl. Phys.,* 8 (2008), 99.

[5] GALICIA D.M.C., CASTANEDO-PEREZ R., JIMENEZ-SANDOVAL O., JIMENEZSANDOVAL S., TORRES-DELGADO G., ZUNIGA-ROMERO C.I., *Thin Solid Films,* 371 (2000), 105.

[6] DONG W., ZHU C., *Opt. Mater.,* 22 (2003), 227.

[7] VINODKUMAR R., LETHY K.J., ARUNKUMAR P.R., KRISHNAN R.R., PILLAI N.V., PILLAI V.P.M., PHILIP R., *Mater. Chem. Phys.,* 121 (2010), 406.

[8] GRADO-CAFFARO M.A., GRADO-CAFFARO M., *Phys. Lett. A,* 372 (2008), 4858.

[9] PAWAR S.M., GURAV K.V., SHIN S.W., CHOI D.S., KIM I.K., LOKHANDE C.D., RHEE J.I., KIM J.H., *J. Nanosci. Nanotechnol.,* 10 (2010), 1.

[10] KUMARAVEL R., MENAKA S., SNEGA S.R.M., RAMAMURTHI K., JEGANATHAN K., *Mater. Chem. Phys.,* 122 (2010), 444.

[11] SUBRAMANYAM T.K., UTHANNA S., NAIDU B.S., *Mater. Lett.,* 35 (1998), 214.

[12] MAITY R., CHATTOPADHYAY K.K., *Sol. Energ. Mat. Sol. C.,* 90 (2006), 597.

[13] LIU X., LI C., HAN S., HAN J., ZHOU C., *Appl. Phys. Lett.,* 82 (2003), 1950.

[14] GUTIERREZ L.R., ROMERO J.J.C., TAPIA J.M.P., CALVA E.B., FLORES J.C.M., LOPEZ M.O., *Mater. Lett.,* 60 (2006), 3866.

[15] BALU A.R., NAGARETHINAM V.S., SUGANYA M., ARUNKUMAR N., SELVAN G., *J. Electron. Devices,* 12 (2012), 739.

[16] KHALLAF H., CHEN C.T., CHANG L.B., LUPAN O., DUTTA A., HEINRICH H., SHENOUDA A., CHOW L., *Appl. Surf. Sci.,* 257 (2011), 9237.

[17] SHINDE V.R., LOKHANDE C.D., MANE R.S., HAN S.H., *Appl. Surf. Sci.,* 245 (2005), 407.

[18] NENOV T.G., YORDANOV S.P., *Ceramic Sensors-Technology and Applications*, Technomic Publishing, USA, 1996.

[19] WINDICHAMANN H., MARK P., *J. Electrochem. Sc.,* 4 (1979), 627.

[20] MIZSEI J., *Sensor. Actuat. B-Chem.,* 23 (1995), 173.

[21] QI Q., ZHANG T., ZHENG X., FAN H., LIU L., WANG R., ZENG Y., *Sensor. Actuat. B-Chem.,* 134 (2008), 36.

[22] GONG J., CHEN Q., LIAN M., LIU N., STEVENSON R.G., ADAMIC F., *Sensor. Actuat. B-Chem.,* 114 (2006), 32.

[23] EGASHIRA M., KAWASUMI S., KAGAWA S., SEIYAMA T., *Bull. Chem. Sc. Jpn.,* 51 (1978), 3144.

[24] MONDAL B., BASUMATARI B., DAS J., ROYCHAUDHURY C., SAHA H., MUKHERJEE N., *Sensor. Actuat. B-Chem.,* 194 (2014), 389.